2024-02-20

Contamination of Thames Estuary sediments by retroreflective glass microbeads, road marking paint fragments and anthropogenic microfibres

West-Clarke, Z

10.1016/j.scitotenv.2023.169257
Science of The Total Environment
Elsevier BV

Science of the Total Environment 912 (2024) 169257

Contents lists available at ScienceDirect

Science of the Total Environment

journal homepage: www.elsevier.com/locate/scitotenv

Contamination of Thames Estuary sediments by retroreflective glass microbeads, road marking paint fragments and anthropogenic microfibres

Zaria West-Clarke, Andrew Turner *

School of Geography, Earth and Environmental Sciences, University of Plymouth, Drake Circus, Plymouth PL4 8AA, UK

HIGHLIGHTS

- Inner Thames Estuary sediment highly contaminated by metals (e.g., Pb, Zn)
- Sediment also contaminated by micro-debris (glass spheres, paint, microfibres)
- Maximum concentrations of spheres and fibres about 28,000 and 60,000 kg^{-1}
- Concentrations exhibited significant, inverse relationship with sediment grain size
- Airborne fibres and debris from road surface washed into Thames with stormwater runoff

GRAPHICAL ABSTRACT

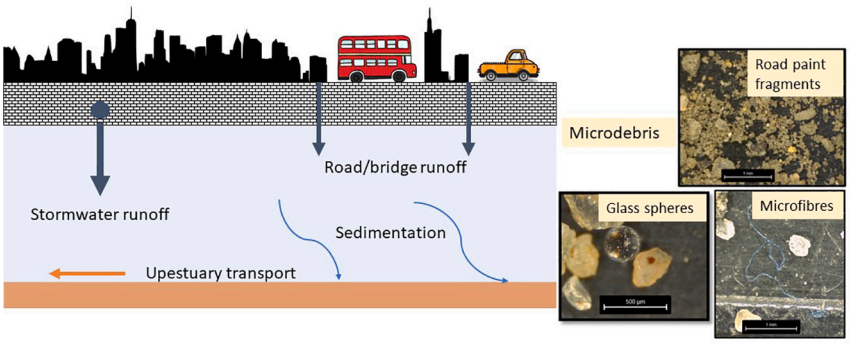

ARTICLE INFO

Editor: Kevin V. Thomas

Keywords:
Pollution
Urban
Microplastics
Lead
Stormwater
Microdebris

ABSTRACT

Surface and subsurface sediment samples ($n = 16$) from the highly urbanised inner Thames Estuary (UK) have been physically and chemically characterised and analysed for anthropogenic microdebris. Sediments were gravelly sands throughout and were heavily contaminated by lead (Pb, up to 12,500 mg kg^{-1}) and zinc (Zn, up to 9500 mg kg^{-1}). Microfibres of mm-dimensions and retroreflective glass microbeads (median diameter = 188 μm) used in road markings were the most abundant types of microdebris present, and concentrations (as numbers, *N*) on a dry weight basis were spatially heterogeneous (ranging from about 4000 to 60,000 *N* kg^{-1} and 100 to 28,000 *N* kg^{-1}, respectively). Nevertheless, concentrations of the two types of particle were significantly correlated and both displayed an inverse, non-linear relationship with sediment grain size. Road marking paint fragments of different colours were detected in most cases ($n = 13$) but quantification was difficult because of analytical constraints related to size, shape, colour, fragmentation and encrustation. Concentrations of up to about 500 mg kg^{-1} Pb were determined in isolated paint fragments but road paint particles are unlikely to make a significant contribution to Pb pollution in Thames Estuary sediments. Overall, our observations suggest that stormwater runoff is a significant source of multiple types of anthropogenic microdebris in urban estuaries, with additional, direct atmospheric deposition contributing to microfibre accumulation. More generally, it is recommended that studies of microplastics consider additional debris and sediment characteristics for a better understanding of their sources and transport.

* Corresponding author.
E-mail address: aturner@plymouth.ac.uk (A. Turner).

https://doi.org/10.1016/j.scitotenv.2023.169257
Received 25 October 2023; Received in revised form 7 December 2023; Accepted 7 December 2023
Available online 19 December 2023

1. Introduction

Microplastics, or plastics in the size range 1 μm to 5 mm, have been subject to intense scientific scrutiny over the past two decades. Although microplastics are ubiquitous throughout the environment, considerable attention has been paid to coastal settings, including estuaries, beaches, wetlands, islands and shelf seas, because of their proximity to primary and secondary waterborne and airborne anthropogenic sources (Leibezeit and Dubaish, 2012; Nel and Froneman, 2015; Stolte et al., 2015; Rose and Webber, 2019; Schröder et al., 2021; Al Nahian et al., 2022; Almeida et al., 2023).

Despite the plethora of studies on microplastics, additional types of microscopic debris have often been overlooked, and in particular in sediment. An example in this regard is the recent interest in rubber tyre particles, which now appear to fall under the umbrella term of microplastics (Leads and Weinstein, 2019; Luo et al., 2021; Klun et al., 2023). However, a variety of other anthropogenic particles that could be defined as or that are unrelated to microplastics has been reported less frequently. The principal reason for their oversight is related to the conventional means of microplastic separation from sediment based on density. Here, a saline solution whose density ranges from about 1.2 to 1.8 g cm^{-3} is used to float out microplastics, with anthropogenic microdebris that is negatively buoyant contained in the settled residue that is generally neglected (Coppock et al., 2017; Quinn et al., 2017). Analysis of the non-floating fraction has, however, revealed the presence of paint fragments, including road marking paints, plastiglomerates, or agglomerates of rock and plastic, and retroreflective glass spheres used in road markings (Horton et al., 2017; Turner and Keene, 2023).

While some residual particles, including paint fragments, could be defined as microplastic based on a common, polymeric matrix, others, like glass microbeads, are clearly inorganic. Nevertheless, consideration of a wider range of microdebris could provide a better understanding of the sources, transport and fate of microplastics in the environment through co-associations or differences. In the urban setting, for example, road marking paint fragments and glass microbeads have a clear primary source and a number of distinctive secondary sources (e.g., road runoff and stormwater discharge).

The aim of the present study is to determine the quantities and evaluate the characteristics and sources of microdebris in sediments from the inner, urbanised Thames Estuary (UK), by direct, microscopic inspection of sieved and dried but otherwise unprocessed samples. We pay particular attention to microfibres, as the most dominant form of microplastics, paint fragments from road markings and retroreflective glass beads, and hypothesise that road runoff represents a significant source of all particle types. We also determine important geochemical characteristics (grain size, organic content) and concentrations of anthropogenic metals (e.g., lead and zinc) in order to investigate the controls on microdebris transport and deposition and their potential contribution to sediment pollution.

2. Methods

2.1. Study area

The Thames Estuary, southern England, has a catchment of about 16,000 km^2 that supports a population of over 13 million (Mitchell et al., 2012). The estuary is well-mixed and macrotidal and extends about 100 km from its landward boundary at Teddington Weir (Fig. 1), where an average freshwater flow rate of 90 m^3 s^{-1} has been recorded, to Nore sandbank in the North Sea (Port of London Authority, 2023). The inner Thames Estuary passes through London and is urbanised and industrialised throughout. It is essentially a canal of about 100 to 300 m in width that is constrained by solid artificial walls (Milne, 1985), with anthropogenic interventions including bridge building, dredging and flood defences (Rossington and Spearman, 2009). Many of its tributaries are also engineered, flowing through either culvert or concrete-steel channels (Catchment Partnerships in London, 2020). The inner estuary is ebb-dominant and supports a turbidity maximum, and sediment, derived from fluvial, marine and anthropogenic (mainly sewage and stormwater) sources, is largely fine and muddy (Rossington and

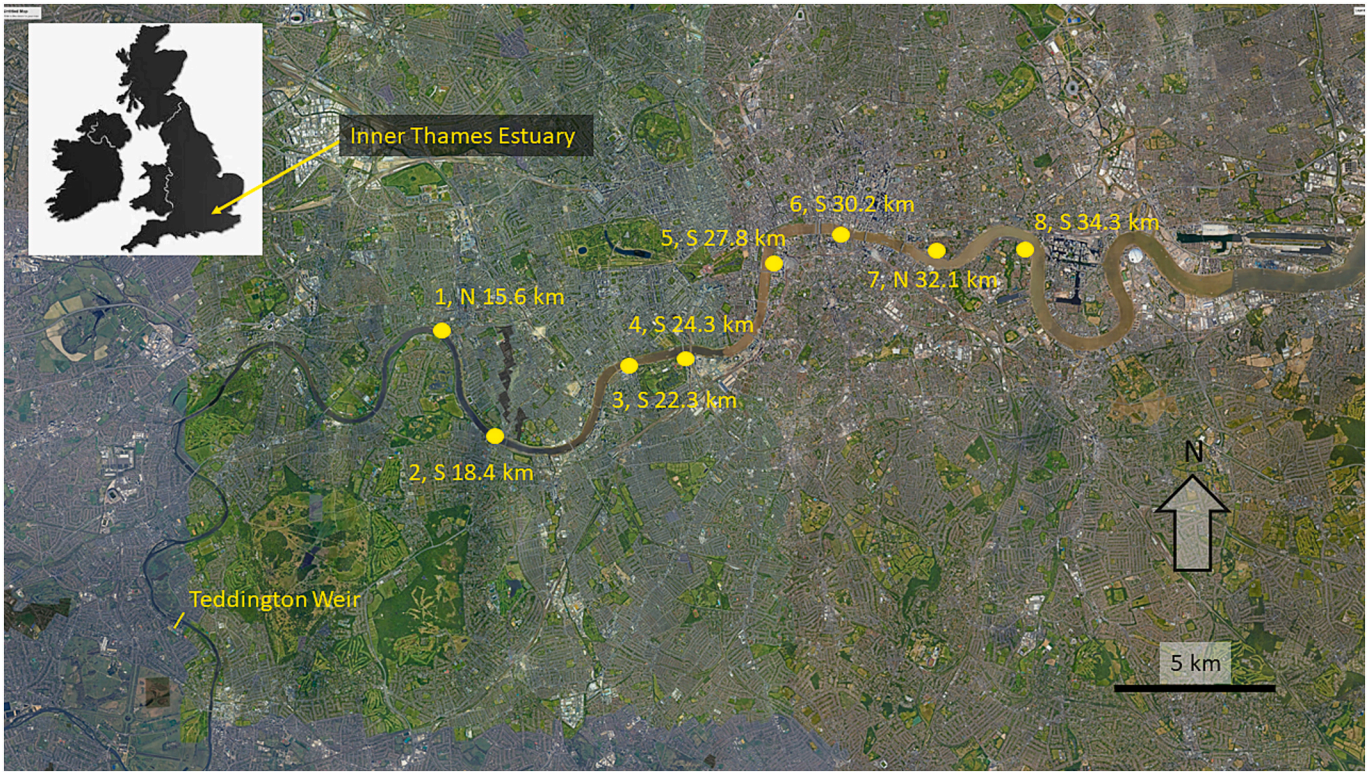

Fig. 1. Sampling locations in the inner Thames Estuary. N or S denotes north or south bank, respectively, and distances are from the tidal weir at Teddington.

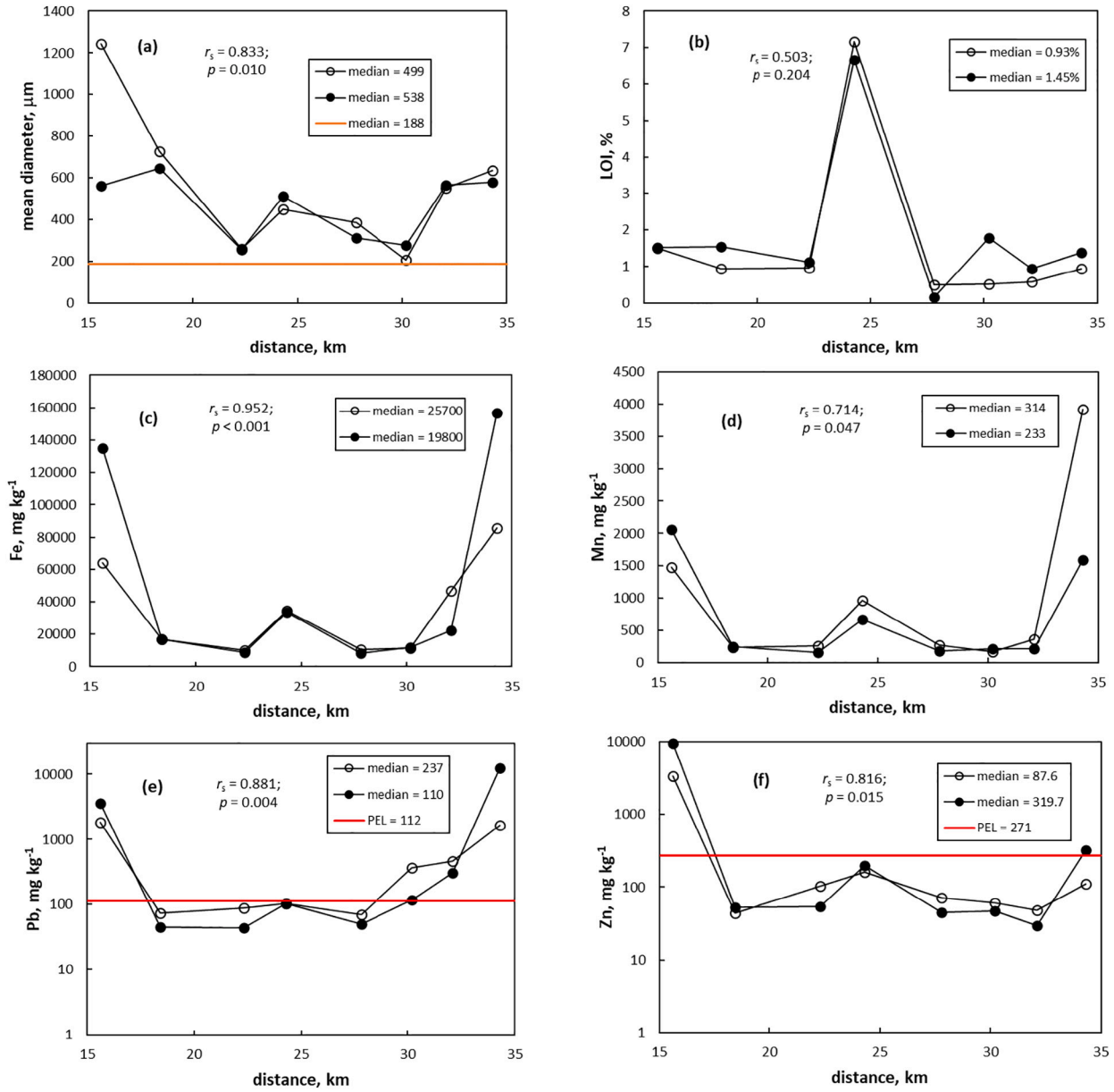

Fig. 2. Axial distributions of characteristics and element concentrations of surface (○) and subsurface (●) sediments (< 5 mm) from the inner Thames Estuary. (a) Mean sediment grain diameter, (b) loss on ignition, (c) concentration of Fe, (d) concentration of Mn, (e) concentration of Pb, and (f) concentration of Zn. Median values and results from Spearman's rank correlation analysis are annotated. Lines parallel to the *x*-axis in orange are the median diameter of glass microbeads (a) and in red are the Canadian Council of Ministers of the Environment (2012) probable effect levels for Pb (e) and Zn (f) in sediment.

Spearman, 2009).

2.2. Sampling

Sediment samples were collected in May 2023 from eight locations in the inner Thames Estuary where access allowed (via steps or slipways) and where sediment was exposed at low tide (Fig. 1). The six most landward locations were close to road bridges and at five locations (2, 3, 6, 7, 8) storm drains were visible. About 50 g of surface (< 1 cm; oxic) and subsurface (5 cm; anoxic) sediment was collected with a stainless-steel trowel and transferred to individual plastic containers (100 mL, screw-capped) that had been pre-lined with aluminium foil before being stored at 4 °C and in the dark pending processing and analysis.

Where evident and readily accessible, fragments of local road marking paints (n = 9) were collected from deteriorating asphalt and concrete surfaces using a pair of stainless-steel tweezers. Samples were stored in individual specimen bags in a sealed plastic box at room temperature.

2.3. Sample processing and microscopic analysis

Sediment samples were sieved through a 5-mm brass mesh with the aid of distilled-deionised water in order to remove large debris. Samples were then dried in foil-covered aluminium trays in an oven at 40 °C for 24 h before being disaggregated with a ceramic pestle and mortar. One g at a time and evenly spread out on a segmented stainless-steel tray, 10 g of dried sediment was analysed under a Leica S9i stereomicroscope with an integrated camera for anthropogenic microdebris that was counted, photographed and sized (with the aid of Leica LASX software). The focus was on retroreflective glass beads (identified according to criteria outlined elsewhere; Turner and Keene, 2023), road marking paint particles (identified based on visible and microscopic characteristics of the 20

Table 1
Summary statistics for various contaminant metals and metalloids in inner Thames estuarine sediment. Also shown are probable effect levels (PELs) according to the Canadian Council of Ministers of the Environment (2012). All units are mg kg^{-1}; na = not available.

	Median-surface, mg kg^{-1}	Median-subsurface, mg kg^{-1}	Min, mg kg^{-1}	Max, mg kg^{-1}	PEL, mg kg^{-1}
As	39.9	80.7	14.2	92.3	41.6
Cr	39.4	42.3	17.4	2260	160
Cu	103	65.8	20.5	867	108
Pb	237	110	43.9	12,500	112
Sb	47.1	47.9	37.5	272	na
Sn	73.9	44.8	23.1	630	na
Zn	87.6	53.3	29.3	9480	271

larger fragments retrieved directly from roadways; see below) and plastic, or, strictly, anthropogenic, microfibres (flexible, individual or intertwined particles with a ratio of length to diameter exceeding ten and identified according to criteria outlined by MERI, 2014). However, other debris (e.g., tyre-wear particulates, plastic fragments and fly ash spheres) was also noted but not quantified because of constraints on identification relating to colour, size and shape distribution, and encrustation on other substrates. In order to check and, if necessary, correct for microfibre contamination in the laboratory, fibre deposition on a filter paper adjacent to the microscope was monitored throughout.

A selection of glass beads ($n = 10$) was also analysed under a JEOL JSM-6610LV scanning electron microscope (SEM) coupled with an Oxford Instruments energy dispersive X-ray (EDX) spectrometer and Aztec software. With the aid of stainless-steel tweezers or a fine (000), wetted

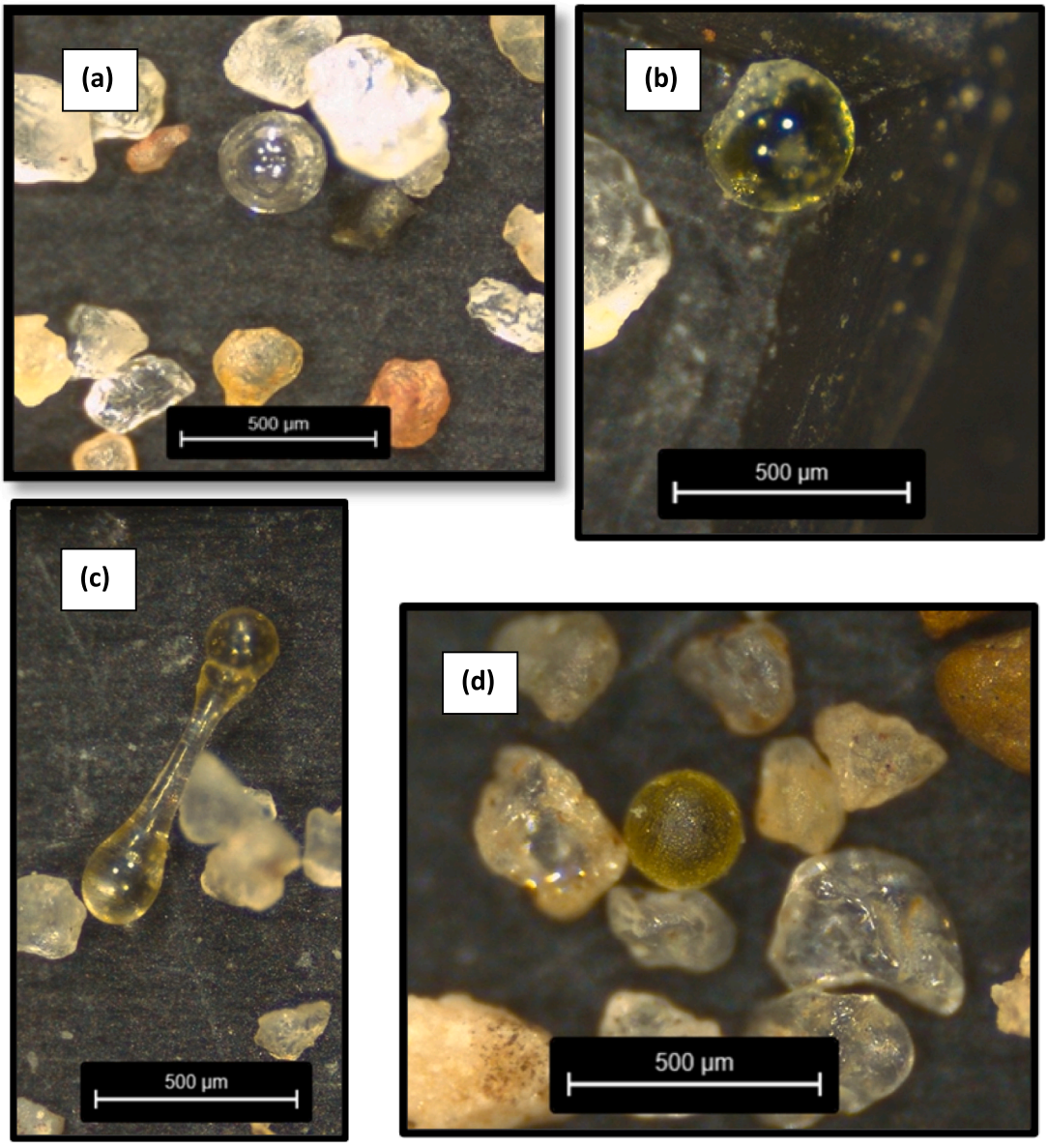

Fig. 3. Examples of glass microbeads retrieved from Thames Estuary sediment. (a) A clear sphere with minor abrasion, (b) a damaged sphere tinted yellow, (c) two beads fused together, presumably during manufacture, and (d) a yellow sphere with a frosted appearance.

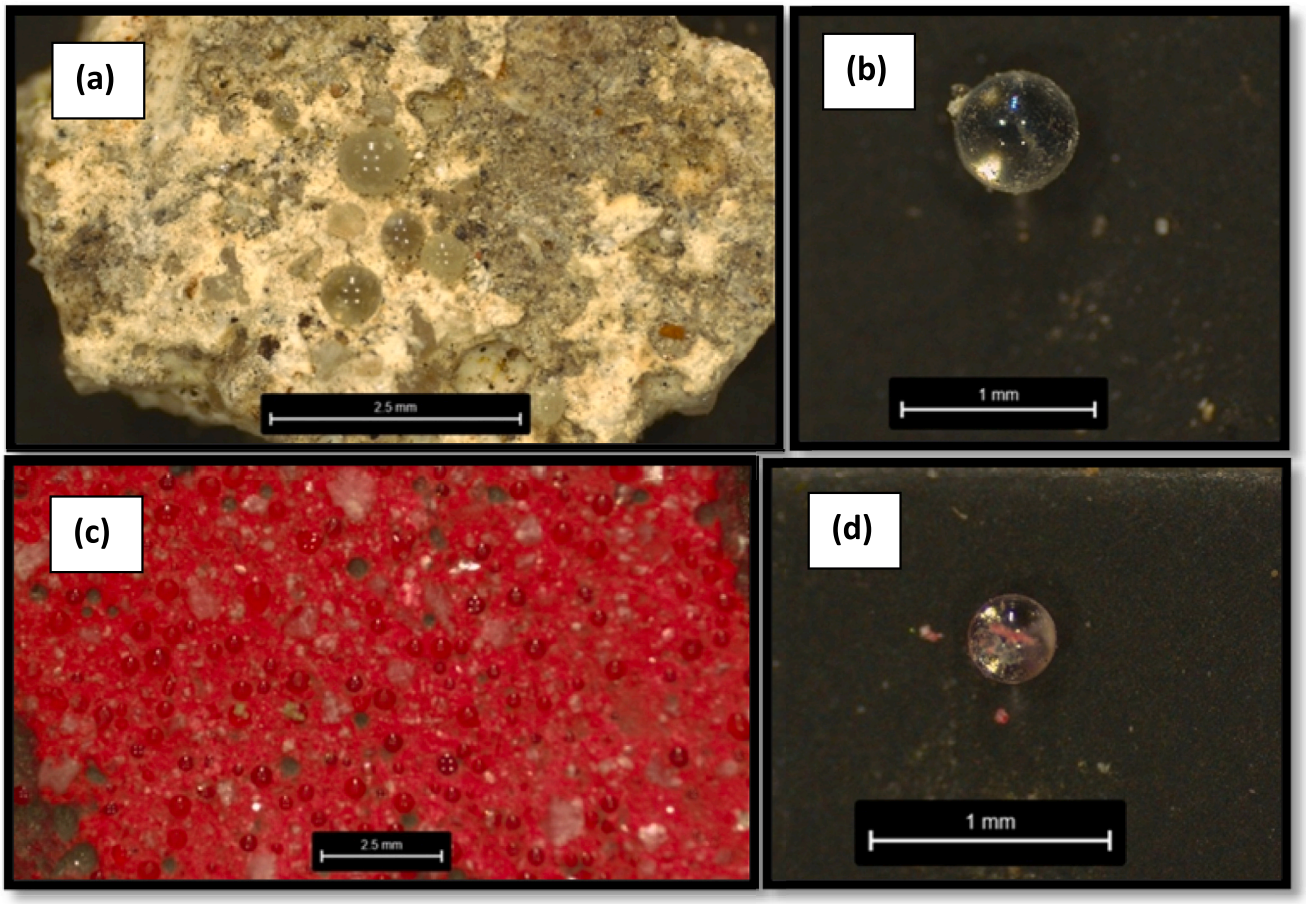

Fig. 4. Examples of glass microbeads within (a and c) and retrieved from (b and d) fragments of local white and red road markings.

paint brush, and under a Leica microscope, beads were removed from the steel tray and mounted on Agar Scientific carbon infiltrated minitabs before being transferred to the SEM that was operated with an accelerating voltage of 15 kV and in a low vacuum mode.

2.4. Sediment, road marking paint fragment and microfibre characterisation

Ten g portions of each dried (< 5 mm) sediment sample were sieved through a series of 14 brass meshes (between 63 μm and 4 mm) and the resulting contents on each sieve were weighed on a Sartorius microbalance. Particle size characteristics were then computed using GRADISTAT, version 9.1 (Kenneth Pye Associates Ltd), a grain size distribution and statistics package originally described by Blott and Pye (2001).

The organic matter content of sediment samples was estimated by weight loss on ignition. Here, about 1 g of dried material was weighed into a ceramic crucible and combusted at 550 °C in a Carbolite AAF1100 furnace for 6 h before the cooled contents were reweighed.

The elemental content of sediment was determined by energy-dispersive X-ray fluorescence (XRF) spectrometry using a field-portable Niton XL3t GOLDD+ housed in a laboratory test stand. About 5 g of each dried sample was transferred to a polyethylene XRF sample cup (Chemplex series 1400; 21-mm internal diameter, 20 mm depth) that was subsequently collar-sealed with 3.6 μm SpectraCertified Mylar polyester film and positioned over the detector window. Measurements were made for 60 s across a range of energies in a mining-soils mode (Turner and Taylor, 2018) and fluorescent counts were converted to concentrations (in mg kg^{-1}) using Niton Data Transfer software. Analysis of a certified reference material (stream sediment GBW07301a; Institute of Geophysical and Geochemical Exploration, Langfang, China) returned concentrations of various elements (including As, Cr, Cu, Fe, Mn, Pb and Zn) that were within 5 to 15 % of certified values.

Road marking paint fragments sampled from the roadside ($n = 9$) and a selection of fragments retrieved from the sediment samples ($n = 13$) were also analysed by the XRF spectrometer in its laboratory stand. Here, individual fragments were suspended on Mylar film directly over the detector window and counted under the operating conditions described above. However, for fragments below the size of the 8-mm X-ray beam, a small spot collimation (to 3 mm) was employed.

A selection of anthropogenic microfibres ($n = 20$) was analysed by Fourier transform-infrared (FTIR) spectroscopy in transmission mode with a Bruker Vertex 70 spectrometer coupled with a Hyperion 1000 microscope. Details of sample preparation and instrument settings are given elsewhere (Kyriakoudes and Turner, 2023).

2.5. Statistics

In Minitab *v*19, an Anderson-Darling test was applied to each dataset to determine normality before appropriate parametric or non-parametric correlations and difference tests were performed with an α-value for significance defined as 0.05. Data fitting and linear and non-linear regression analysis was performed in Excel 365.

3. Results

3.1. Sediment characteristics

Particle size analysis revealed that both surface (oxic) and subsurface (anoxic) sediments from the inner Thames Estuary were poorly- to well-

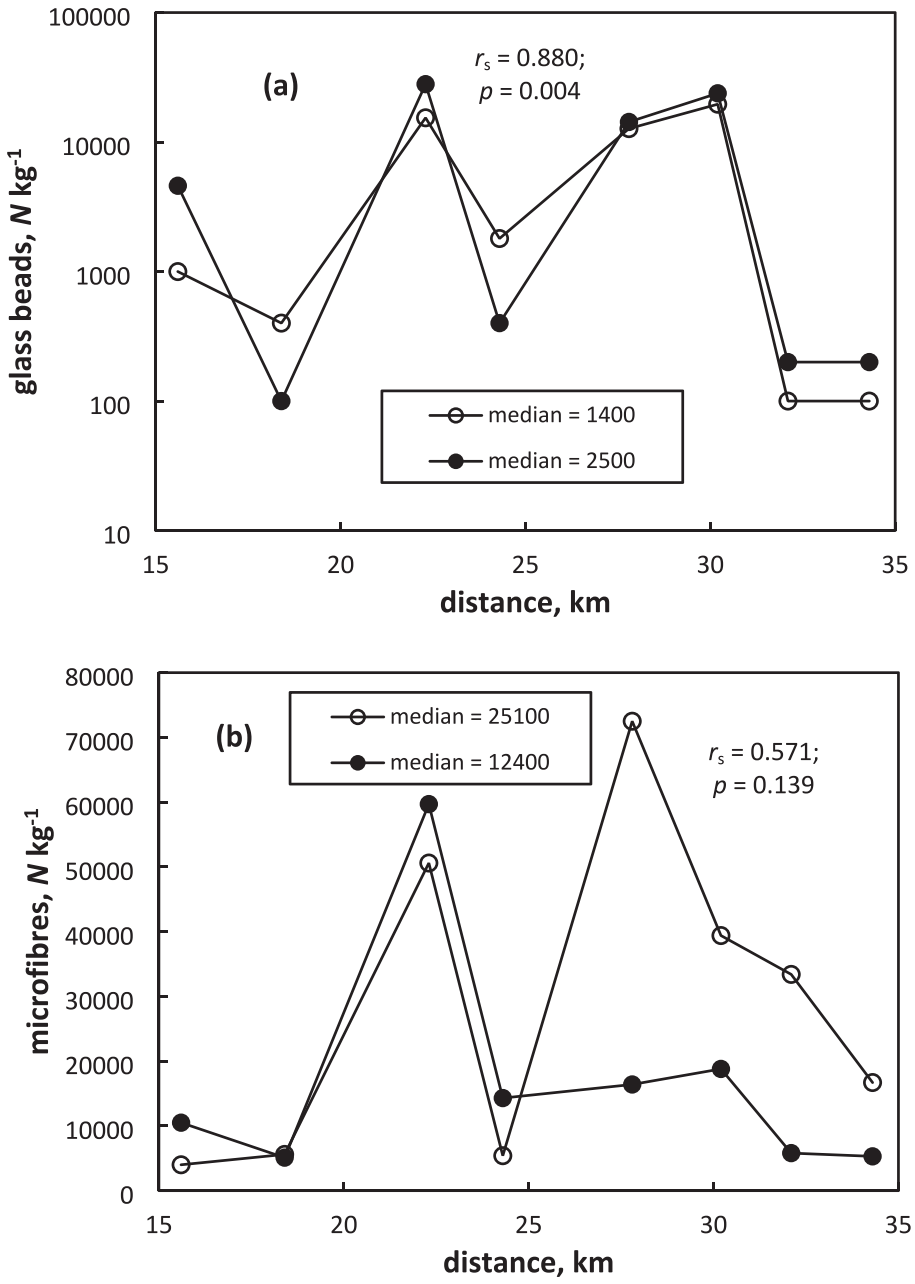

Fig. 5. Concentrations of (a) glass microbeads and (b) anthropogenic microfibres as a function of axial distance in surface (○) and subsurface (●) sediments (< 5 mm) from the inner Thames Estuary. Median values and results from Spearman's rank corelation analysis are annotated.

sorted "gravelly sands", being dominated by sand (63 to 2000 μm; > 75 %) and with smaller proportions of gravel (above 2000 μm; < 20 %) and silt (below 63 μm; < 3 %).

The characteristics of the surface and subsurface Thames sediment, along with the concentrations of a selection of geochemically relevant elements (Fe and Mn) and contaminant metals (Pb and Zn), are shown in Fig. 2 as a function of axial distance downestuary from the tidal weir. Also shown for Pb and Zn are the respective probable effect levels (PELs) at which adverse effects frequently occur according to the Canadian Council of Ministers of the Environment (2012). (Note that Table 1 provides summary statistics for a broader suite of metals and metalloids.) Among the variables, there are no clear axial trends, but the distributions of a given variable are similar at the surface and subsurface. Consequently, there were no significant differences between median values at the two depths according to a series of Wilcoxon signed rank tests, but surface and subsurface data were usually significantly correlated (and as annotated). Note that correlations between different variables at either depth were not significant.

3.2. Abundance and characteristics of microdebris

3.2.1. Glass microbeads

A total of 1236 solid, non-plastic microbeads were identified under the light microscope in the sixteen (10-g) sediment samples from the Thames, with examples shown in Fig. 3. Most were clear (transparent), colourless and spherical, with varying degrees of abrasion evident; however, some were coloured white or yellow, presumably from the original paint matrix, misshapen or fused during manufacture, or damaged by weathering or impact. For comparison, Fig. 4 illustrates microbeads within or retrieved directly from road markings. Here, spherical beads were present in all marking colours inspected, but were least frequently observed in yellow samples. In situ, microbeads

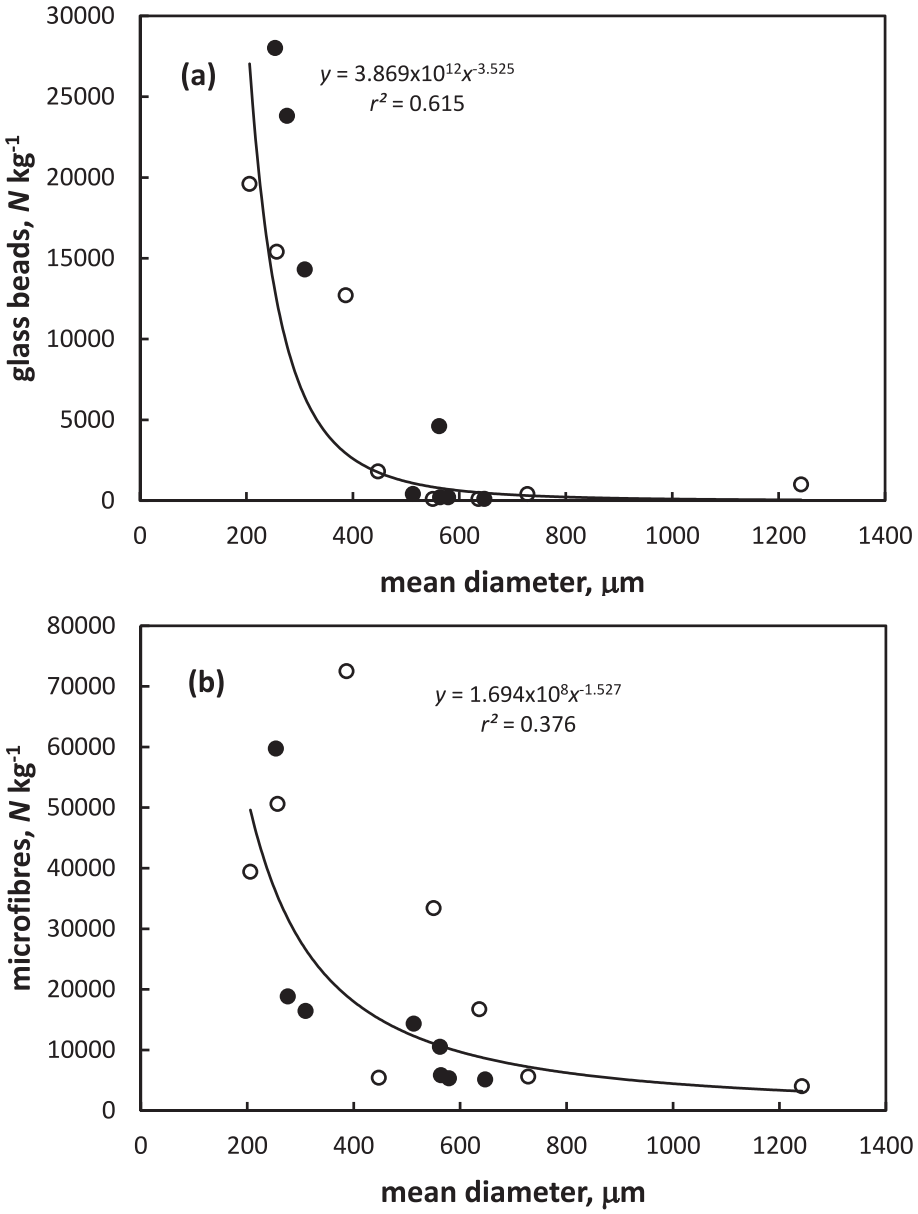

Fig. 6. Concentrations of (a) glass microbeads and (b) anthropogenic microfibres as a function of mean grain diameter in surface (○) and subsurface (●) sediments (< 5 mm) from the inner Thames Estuary. Annotated are the best-fit power-law regressions and their equations.

appeared to take on the colour of the marking but when isolated were clear, with some visibly contaminated by coloured paint particulates derived from the marking matrix. SEM-EDX analysis of a selection of beads retrieved from sediment and road markings confirmed a glass matrix (with strong signals of Si, Ca and Na), and the presence of additional contaminants at the glass surface (e.g., Fe and Ti).

Concentrations of retroreflective glass microbeads in Thames Estuary sediment (number, *N*, per kg dry weight) are shown as a function of axial distance in Fig. 5a. Beads were detected in all samples, with concentrations ranging from 100 to 28,000 *N* kg^{-1}. As above, median concentrations were not significantly different between surface and subsurface samples but concentrations at the two depths were significantly correlated. Concentrations were also inversely related to sediment grain diameter (Fig. 6); specifically, logged values were significantly correlated and original data were defined by a non-linear power-regression of the form: $y = ax^{-b}$.

The size distribution of all glass microbeads retrieved from Thames Estuary sediment is shown in Fig. 7, along with a summary of descriptive statistics. Note that while size data exist for microbeads from each sediment sample, in five cases these relied on the measurement of just one or two beads. Overall, diameters ranged from about 20 (the approximate detection limit for this type of particle) to 950 µm, with the majority (93.3 %) between 100 and 300 µm. Most beads, therefore, fall in the fine to medium sand size category, and the overall median diameter of 188 µm is lower than the median sediment grain diameter at each location (Fig. 2a). Based on spherical geometry and a density of glass of 2.5 g cm^{-3}, the median diameter is equivalent to a median bead mass of about 9 µg. On this basis, therefore, estimated bead concentrations on a dry mass basis range from about 1 to 250 mg kg^{-1} in the Thames Estuary sediment samples.

3.2.2. *Road marking paint fragments*

Fragmented particles of road marking paint observed in Thames Estuary sediment are exemplified in Fig. 8. In a few cases (e.g., Fig. 8c), markings of about 1 mm or greater appeared to be attached to a substrate, but otherwise discrete fragments of various sizes were evident.

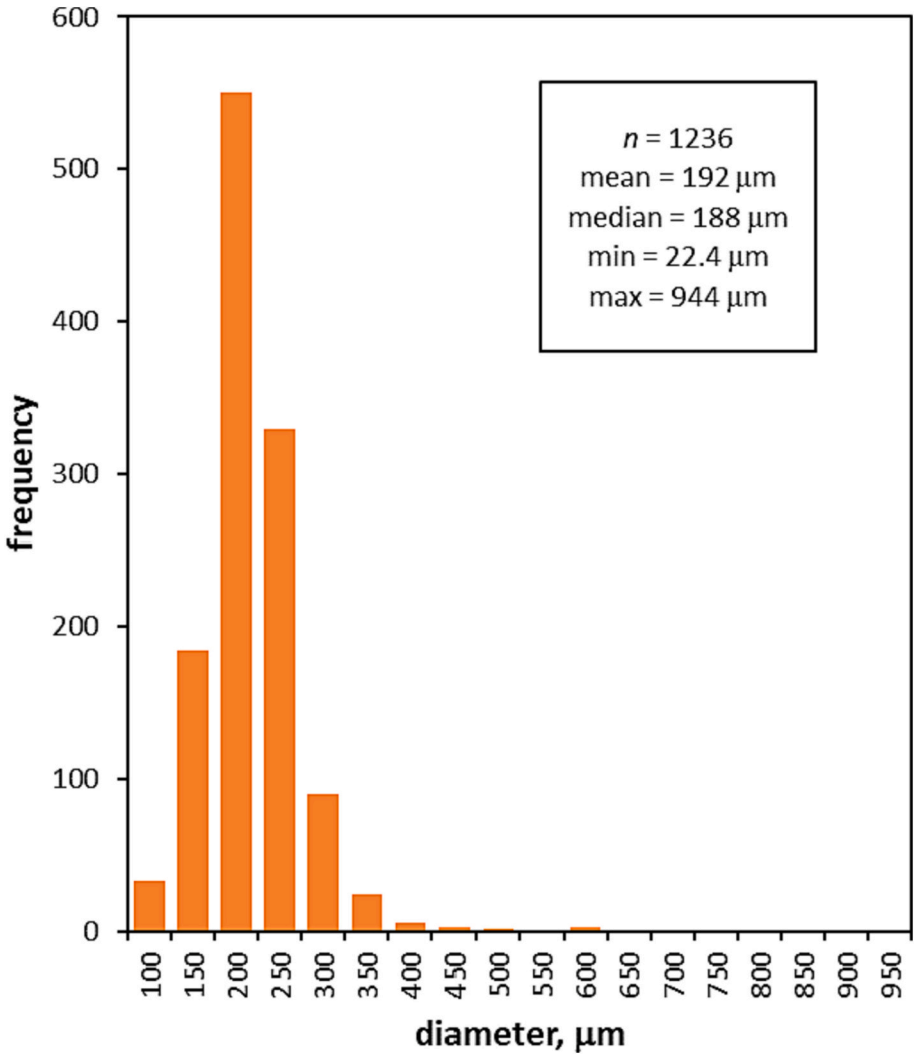

Fig. 7. Size distribution of and descriptive statistics for glass microbeads in Thames Estuary sediment.

Because of the ready fragmentation of some discrete particles during manipulation under the microscope, it was surmised that the abundance of relatively small particles in some samples (e.g., Fig. 8b) reflected the fragmentation of fewer, larger particles. It is also suspected that, because of similarities with natural silt and shell particles, the quantities of white and yellow fragments, and in particular those below 100 µm in size, were underestimated compared with red and blue fragments. For these reasons, road marking particles were not quantified in sediment samples on a number basis; rather, their presence or absence by colour was noted. Accordingly, fragments were detected in sediments from all locations with the exception of site 2, and at both surface and subsurface samples with the further exception of site 1 (surface only). By colour, red, yellow and white were most commonly detected (11, 10 and 9 cases each, respectively) and blue was found least frequently (five cases). All colours were represented in surface sediments at sites 5, 6 and 7.

Results arising from XRF analysis of individual road marking paint fragments sampled directly from the road and retrieved from estuarine sediments are shown in Table 2. Here, all colours are included in both sample types and data are shown for elements that are or have been employed in road paint pigments. Absolute concentrations are subject to some uncertainty (underestimation) where part of the underlying substrate was included but results reveal similar median concentrations of Ti and Zn in the two sample types, and greater median concentrations (and/or more detects) of Cr, Fe and Pb in samples retrieved from sediment.

There was no clear relationship between glass microbead abundance and the presence of road marking paint fragments in sediment. For example, the absence of road marking paints was noted where glass bead abundance ranged from 100 $N\ kg^{-1}$ (site 2, subsurface) to 15,400 $N\ kg^{-1}$ (site 3, surface), and all colours of road marking paints were observed where glass bead concentrations ranged from 100 $N\ kg^{-1}$ (site 7, surface) to 19,400 N kg^{-1} (site 6, surface).

3.2.3. *Anthropogenic microfibres*

A total of about 3600 anthropogenic microfibres were counted among the sediment samples. Because of such a large number, along with other debris considered, the precise sizes and colours of all fibres were not recorded. However, an inspection of photographs taken, and exemplified in Fig. 9, revealed lengths between about 100 µm (the approximate detection limit under the microscope) and 5 mm and colours that were mainly black, blue, red and white. FTIR analysis of 20 fibres revealed that the majority were cellulosic (i.e., non-petroleum-based), and of these the main polymer was rayon.

Concentrations of anthropogenic microfibres in Thames Estuary sediment ranged from about 4000 to 72,500 $N\ kg^{-1}$ and are shown as a function of axial distance in Fig. 5b. Median concentrations were not significantly different between surface and subsurface samples and the correlation between concentrations at the two depths was not significant. Fibre concentrations appeared to be inversely related to sediment grain diameter (Fig. 6b) but the correlation between logged values was

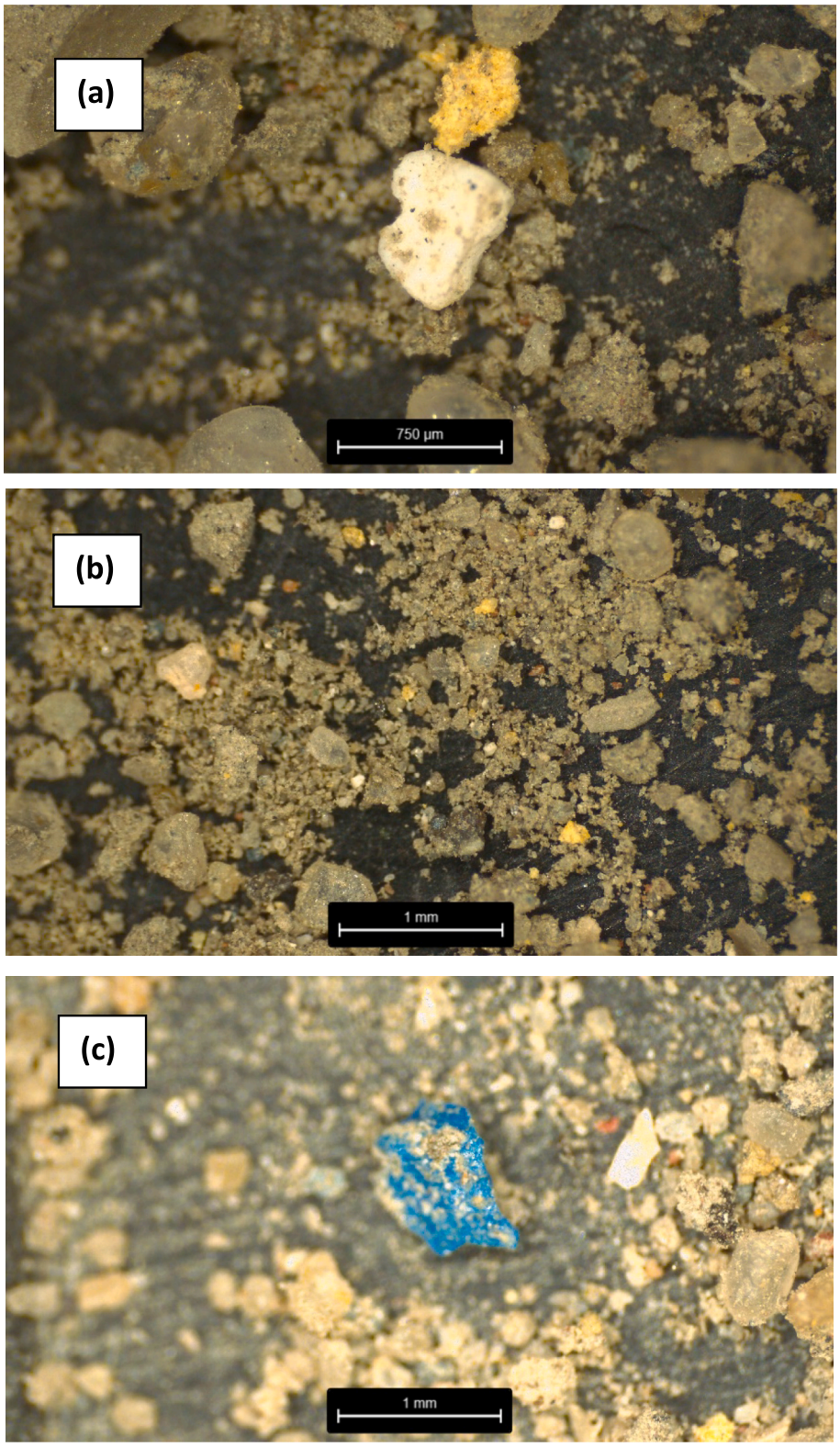

Fig. 8. Examples of road marking fragments observed in <5 mm sediments from the inner Thames Estuary. (a) A white and yellow fragment below 750 µm in size, (b) multiple yellow fragments ranging in size from <50 µm to about 200 µm, and (c) a mm-sized blue fragment that appears to be attached to its substrate.

not significant. However, a significant correlation was established between the concentrations of microfibres and glass beads in all sediment samples ($r_s = 0.544; p = 0.030$), with a best-fit linear regression equation of: $y = 1.488x + 11{,}300$.

4. Discussion

Elevated levels of chemical pollutants, including persistent organic compounds and heavy metals, are a reflection of the contamination of inner Thames Estuary sediment arising from a variety of both historical

Table 2
Number of cases in which Cr, Fe, Pb and Zn were detected in road marking paint fragments sampled from the roadside and estuarine sediment, and summary statistics for their concentrations. LOD represents an indictive limit of detection.

	n detected	LOD, mg kg^{-1}	median, mg kg^{-1}	min, mg kg^{-1}	max, mg kg^{-1}
Roadside ($n = 9$)					
Cr	0	5			
Fe	9	50	224	68.1	3330
Pb	0	20			
Ti	9	10	543	13.8	2540
Zn	6	20	62.3	21.2	210
Sediment ($n = 12$)					
Cr	6	10	24.5	18.8	28.0
Fe	9	120	4280	177	12,200
Pb	7	10	90.0	12.2	530
Ti	8	30	158	41.2	2270
Zn	4	10	51.5	10.8	260

and contemporary sources (Scrimshaw and Lester, 1995; Pope and Langston, 2011). The axial heterogeneity in contaminant metal concentrations (e.g., Pb, Zn) likely reflects a diversity of point and diffuse inputs coupled with variations in sediment characteristics (grain size, surface area, hydrous Fe-Mn oxide concentration, organic matter content), while similar metal concentrations at the surface and subsurface may be attributed to the persistence of metal sources over time or the reworking and mixing of sediments in the vertical. One important source of metals and other contaminants in urban estuaries is road runoff that captures a variety of traffic-related pollutants. The significance of this source in sediment may be quantified by the abundance of retroreflective glass microbeads employed in road markings (Zannoni et al., 2016).

Although glass microbeads have been reported in various aquatic systems previously, including in several freshwater tributaries of the Thames (Horton et al., 2017), quantitative information is very limited. Specifically, Migaszewski et al. (2022) report concentrations in (presumably) surface sediments from rivers in Kielce, southcentral Poland, of up to about 50,000 *N* kg^{-1} in the vicinity of a stormwater drain (median = 120 *N* kg^{-1}; $n = 30$), while Turner and Keene (2023) determined concentrations up to about 550 *N* kg^{-1} in intertidal surface and subsurface sediments from the lower, and partly urbanised, Tamar Estuary, southwest England (median = 254 *N* kg^{-1}; $n = 9$). By comparison, the present study has revealed a maximum concentration of 28,000 *N* kg^{-1} in surface and subsurface intertidal sediments from the Thames Estuary, with a median concentration of about 2000 *N* kg^{-1} ($n = 16$). The high variability of glass microbead concentrations in the Thames (with a range spanning more than two orders of magnitude) might result from different sample distances to various sources (stormwater drains, roadways and road bridges), coupled with variations in the magnitude of the sources that relate to the degree (and type and condition) of road marking coverage and traffic wear within the drainage area or local road surface. More generally, however, the inverse relationship between microbead abundance and median sediment grain size (Fig. 6a) suggests that, in the longer term, beads are redistributed in the estuary with fine, silty sediments through tidal currents and dredging activities (Uncles and Mitchell, 2011; Port of London Authority, 2023). Specifically, the

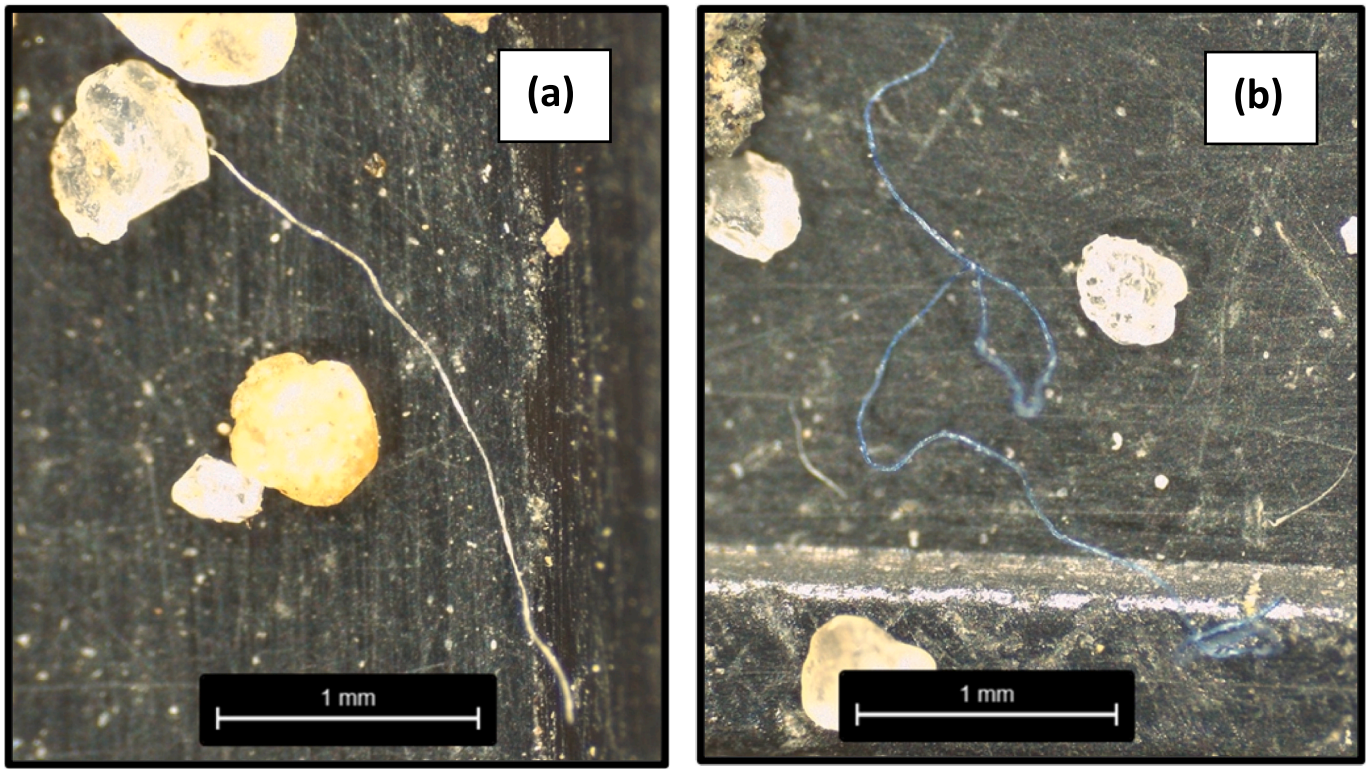

Fig. 9. Examples of microplastic fibres retrieved from (a) surface and (b) subsurface sediment (<5 mm) from the inner Thames Estuary.

asymmetrical tidal currents in the inner estuary are predicted to transport beads upestuary (Brew, 2004).

The present paper appears to be the first to document the presence (and variety) of road marking paint fragments in estuarine sediments. Despite paint fragments and glass microbeads having a common origin, however, there is no clear relationship between or co-existence of the two types of particle. Burkhardt et al. (2023) suggest that the erosion and mobility of beads and paint fragments in road markings are decoupled in that the presence of beads protects the underlying matrix and once the surface layer of beads is damaged or removed, the road marking is usually renewed and not replaced. The authors conclude that the lack of road marking fragments reported in the aquatic environment reflect the protective role of glass microbeads, but also note the lack beads reported in the environmental literature. We contend that the limited observations of these particulates reflects the typical means of sample processing, especially when microplastics are the target of research. Here, microplastics are floated out of the sample in a saturated salt solution whose density is usually around 1.2 to 1.5 g cm^{-3} (e.g., NaCl or $ZnCl_2$; Stolte et al., 2015; Abidli et al., 2017; Rodrigues et al., 2020; Cutroneo et al., 2021) before microscopic inspection and characterisation. The higher densities of road marking paints and glass beads would ensure that they are retained with settled sediment or soil and evade detection (Turner, 2021; Turner and Keene, 2023). Given the ready fragmentation of older road paint particles in situ and when manipulated under the microscope, we also surmise that many paint particles within sediments are too small to be detected and are more widely dispersed with residual and tidal currents. Moreover, detection is made more challenging for paint particles whose colours closely resemble natural (e.g., mineral and shell) particulates.

With the potential for incorporation of road paint fragments into sediments, an important question is whether significant quantities of metallic contaminants from the paint are also introduced. In this respect, the metals of greatest concern are Pb and Cr(VI) that have been employed in the yellow-orange pigment, lead chromate (Adachi and Tainosho, 2004; White et al., 2014). The coloured markings sampled from the roadside and analysed by XRF revealed the presence of various metals but no detectable Pb and (total) Cr. This reflects the recent (albeit complex) restrictions on the use of lead chromate in road paints in Europe (Turner and Filella, 2022). Within the sediment, however, the analysis of isolated road marking fragments revealed the frequent detection of both Pb and (total) Cr, suggesting that older markings are a source of these metals to the environment. In the inner Thames Estuary, at least, the magnitude of this source relative to other anthropogenic sources is likely to be small. For example, the maximum concentration of Pb in road marking paint is about 500 mg kg^{-1}, meaning that contamination of sediment by 1 % of these particles on a weight basis would only contribute around 5 mg kg^{-1} to the total Pb content (the overall median value for Pb in sediment in the present study was about 200 mg kg^{-1}).

Regarding microfibres, a similar distribution with respect to sediment grain size as glass microbeads (Fig. 6b) and a direct correlation between microfibre and microbead concentrations in sediments suggests a common source and means of transport. That is, microfibres appear to be washed into the inner Thames Estuary with stormwater runoff and via road splash and subject to subsequent deposition and estuarine transport with fine, silty sediment. This is in agreement with conclusions of recent studies conducted in other urban areas that stormwater runoff is a highly significant transporter of microplastics to aquatic habitats (Werbowski et al., 2021; Ross et al., 2023). The positive intercept of the regression between microfibre and microbead concentrations (about 11,000 N kg^{-1}) also suggests that there is an additional and more diffuse, non-runoff-related source of microfibres to the estuary. This could be the River Thames at the head of the estuary or direct and persistent atmospheric deposition throughout the estuarine surface.

5. Conclusions

Sediments of the inner Thames Estuary are known to be highly contaminated by chemical pollutants (including metals) but this study has shown that contamination extends to various forms of microdebris. Most abundant in this respect are microfibres and glass microbeads, with road marking paint fragments also detected but likely underestimated because of analytical constraints. Relationships between the variables studied suggest that much microdebris is derived from stormwater effluents and is subject to the hydrodynamic controls that act on fine sediment. In the Thames Estuary, asymmetrical tidal currents result in the upstream transport of particulate matter. A general recommendation is that environmental studies of microplastics also engage other forms of microdebris and sediment characteristics in order to better understand their transport, behaviour and fate.

CRediT authorship contribution statement

Zaria West-Clarke: Data curation, Formal analysis, Methodology, Validation, Writing – original draft. **Andrew Turner:** Conceptualization, Formal analysis, Investigation, Project administration, Supervision, Validation, Writing – original draft, Writing – review & editing.

Declaration of competing interest

The authors declare that they have no known competing financial interests or personal relationships that could have appeared to influence the work reported in this paper.

Data availability

Data will be made available on request.

Acknowledgements

We thank Dr. Jodie Fisher, Mr. Richard Hartley and Mr. Glenn Harper for technical assistance throughout the study.

References

Abidli, S., Toumi, H., Lahbib, Y., El Menhif, N.T., 2017. The first evaluation of microplastics in sediments from the Complex Lagoon-Channel of Bizerte (Northern Tunisia). Water Air Soil Pollut. 228, 262.

Adachi, K., Tainosho, Y., 2004. Characterization of heavy metal particles embedded in tire dust. Environ. Int. 30, 1009–1017.

Al Nahian, S., Rakib, M.R.J., Haider, S.M.B., Kumar, R., Mohsen, M., Sharma, P., Khandaker, M.U., 2022. Occurrence, spatial distribution, and risk assessment of microplastics in surface water and sediments of Saint Martin Island in the Bay of Bengal. Mar. Pollut. Bull. 179, 113720.

Almeida, C.M.R., Sáez-Zamacona, I., Silva, D.M., Rodrigues, S.M., Pereira, R., Ramos, S., 2023. The role of estuarine wetlands (saltmarshes) in sediment microplastic retention. Water 15, 1382.

Blott, S.J., Pye, K., 2001. GRADISTAT: a grain size distribution and statistics package for the analysis of unconsolidated sediments. Earth Process. Landf. 26, 1237–1248.

Brew, D., 2004. Thames Estuary 2100 – Geomorphology Review and Conceptual Model. A Report by the Environment Agency (Thames Region). Royal Haskoning Ltd, Peterborough, UK.

Canadian Council of Ministers of the Environment, 2012. Canadian Environmental Quality Guidelines and Summary Table. http://www.ccme.ca/accessed12/2022.

Catchment Partnerships in London, 2020. River Restoration in London: A 20 Year Review.

Coppock, R.L., Cole, M., Lindeque, P.K., Queirós, A.M., Galloway, T.S., 2017. A small-scale, portable method for extracting microplastics from marine sediments. Environ. Pollut. 230, 829–837.

Cutroneo, L., Reboa, A., Geneselli, I., Capello, M., 2021. Considerations on salts used for density separation in the extraction of microplastics from sediments. Mar. Pollut. Bull. 166, 112216.

Horton, A.A., Svendsen, C., Williams, R.J., Spurgeon, D.J., Lahive, E., 2017. Large microplastic particles in sediments of tributaries of the River Thames, UK – abundance, sources and methods for effective quantification. Mar. Pollut. Bull. 114, 218–226.

Klun, B., Rozman, U., Kalciková, G., 2023. Environmental aging and biodegradation of tire wear microplastics in the aquatic environment. J. Environ. Chem. Eng. 11, 110604.

Kyriakoudes, G., Turner, A., 2023. Suspended and deposited microplastics in the coastal atmosphere of southwest England. Chemosphere 343, 140258.
Leads, R.R., Weinstein, J.E., 2019. Occurrence of tire wear particles and other microplastics within the tributaries of the Charleston Harbor Estuary, South Carolina, USA. Mar. Pollut. Bull. 145, 569–582.
Leibezeit, G., Dubaish, F., 2012. Microplastics in beaches of the East Frisian Islands Spiekeroog and Kachelotplate. Bull. Environ. Contam. Toxicol. 89, 213–217.
Luo, Z.X., Zhou, X.Y., Su, Y., Wang, H.M., Yu, R.L., Zhou, S.F., Xu, E.G., Xing, B.S., 2021. Environmental occurrence, fate, impact, and potential solution of tire microplastics: similarities and differences with tire wear particles. Sci. Total Environ. 795, 148902.
MERI, 2014. Guide to Microplastic Identification. Marine & Environmental Research Institute, Blue Hill, ME, USA.
Migaszewski, Z.M., Gałuszka, A., Dołęgowska, S., Michalik, A., 2022. Abundance and fate of glass microspheres in river sediments and roadside soils: lessons from the Świętokrzyskie region case study (southcentral Poland). Sci. Total Environ. 821, 153410.
Milne, G., 1985. The Port of Roman London. Batsford Ltd.
Mitchell, S., Akesson, L., Uncles, R., 2012. Observations of turbidity in the Thames Estuary, United Kingdom. Water Environ. J. 26, 511–520.
Nel, H.A., Froneman, P.W., 2015. A quantitative analysis of microplastic pollution along the south-eastern coastline of South Africa. Mar. Pollut. Bull. 101, 274–279.
Pope, N., Langston, W.J., 2011. Sources, distribution and temporal variability of trace metals in the Thames Estuary. Hydrobiologia 672, 49–68.
Port of London Authority, 2023. Physical processes. In: https://www.pla.co.uk/Environment/Physical-Processes.
Quinn, B., Murphy, F., Ewins, C., 2017. Validation of density separation for the rapid recovery of microplastics from sediment. Anal. Methods 9, 1491–1498.
Rodrigues, M.O., Gonçalves, A.M.M., Gonçalves, F.J.M., Abrantes, N., 2020. Improving cost-efficiency for MPs density separation by zinc chloride reuse. MethodsX 7, 100785.
Rose, D., Webber, M., 2019. Characterization of microplastics in the surface waters of Kingston harbour. Sci. Total Environ. 664, 753–760.
Ross, M.S., Loutan, A., Groeneveld, T., Molenaar, D., Kroetch, K., Bujaczek, T., Kolter, S., Moon, S., Huynh, A., Khayam, R., Franczak, B.C., Camm, E., Arnold, V.I., Ruecker, N. J., 2023. Estimated discharge of microplastics via urban stormwater during individual rain events. Front. Environ. Sci. 11, 1090267.
Rossington, K., Spearman, J., 2009. Past and future evolution in the Thames Estuary. Ocean Dyn. 59, 1–16.
Schröder, K., Kossel, E., Lenz, M., 2021. Microplastic abundance in beach sediments of the Kiel Fjord, Western Baltic Sea. Environ. Sci. Pollut. Res. 28, 26515–26528.
Scrimshaw, M.D., Lester, J.N., 1995. Organochlorine contamination in sediments of the inner Thames Estuary. J. Chartered Inst. Water Environ. Manag. 9, 519–525.
Stolte, A., Forster, S., Gerdts, G., Schubert, H., 2015. Microplastic concentrations in beach sediments along the German Baltic coast. Mar. Pollut. Bull. 99, 216–229.
Turner, A., 2021. Paint particles in the marine environment: an overlooked component of microplastics. Water Res. X 12, 100110.
Turner, A., Filella, M., 2022. Lead and chromium in European road pints. Environ. Pollut. 316, 120492.
Turner, A., Keene, J., 2023. Glass microbeads in coastal sediments as a proxy for traffic-related particulate contamination. Mar. Pollut. Bull. 188, 114663.
Turner, A., Taylor, A., 2018. On site determination of trace metals in estuarine sediments by field-portable-XRF. Talanta 190, 498–506.
Uncles, R.J., Mitchell, S.B., 2011. Turbidity in the Thames Estuary: how turbid do we expect it to be? Hydrobiologia 672, 91–103.
Werbowski, L.M., Gilbreath, A.N., Munno, K., Zhu, X., Grbic, J., Wu, T., Sutton, R., Sedlak, M.D., Deshpande, A.D., Rochman, C.M., 2021. Urban stormwater runoff: a major pathway for anthropogenic particles, black rubbery fragments, and other types of microplastics to urban receiving waters. ACS ES&T Water 1, 1420–1428.
White, K., Detherage, T., Verellen, M., Tully, J., Krekeler, M.P.S., 2014. An investigation of lead chromate (crocoite-PbCrO4) and other inorganic pigments in aged traffic paint samples from Hamilton, Ohio: implications for lead in the environment. Environ. Earth Sci. 71, 3517–3528.
Zannoni, D., Valotto, G., Visin, F., Rampazzo, G., 2016. Sources and distribution of tracer elements in road dust: the Venice mainland case of study. J. Geochem. Explor. 166, 64–72.